Electronic Structure and Reactivity of the $F_S(H)^+$ Defect Center at the MgO (001) Surface

Raffaella Soave,[†] Anna Maria Ferrari,*[,‡] and Gianfranco Pacchioni[†]

Dipartimento di Scienza dei Materiali, Università di Milano-Bicocca e Istituto Nazionale per la Fisica della Materia, Via R. Cozzi, 53, 20125 Milano, Italy, and Dipartimento di Chimica IFM, Università di Torino, Via P. Giuria 5, 10125 Torino, Italy

Received: May 3, 2001

$F_S(H)^+$ centers (oxygen vacancies with a trapped electron and a nearby hydroxyl group) at the (001) surface of MgO have been characterized in terms of electronic structure, magnetic properties, and chemical reactivity toward adsorption of O_2 and N_2 molecules by means of cluster model density functional calculations. Two different arrangements of the OH group on the surface have been considered: the computed properties are in excellent agreement with observed EPR and IR data and show the existence of important analogies between the two arrangements (e.g., a similar polarization of the spin density), but also of some significant differences (e.g., for one kind of $F_S(H)^+$, a special interaction between the OH group and the trapped electron has been detected). At short distances from the surface, a transfer of the trapped electron from the surface to the admolecules occurs, with formation of charge-transfer complexes $F_S(H)^{2+}/N_2^-$ or $F_S(H)^{2+}/O_2^-$. While $F_S(H)^{2+}/O_2^-$ is stable even at room temperature with respect to dissociation into $F_S(H)^+ + O_2$ fragments, and $F_S(H)^{2+}/N_2^-$ is a metastable surface complex.

1. Introduction

In recent years, there has been rapidly increasing interest in the theoretical and experimental modeling of oxide surface defectiveness, in particular in the case of ionic crystals of alkali halides and alkali-earth oxides.[1−7] In several cases, theory has provided an important complement to the experimental information, furnishing useful tools for a comprehensive understanding of the complex surface reactivity of these materials. It is believed that most of the chemistry occurring on oxide surfaces is determined by the activity of the defect sites, including low-coordinated sites, surface vacancies, divacancies, and impurity atoms,[8] where the symmetry is lower than in the bulk. At these sites important interactions may take place between the surface trapped electrons and molecules adsorbed on the surface from the gas or liquid phases.[9−11] In some cases, an intriguing chemical reactivity, which involves electron transfer from the solid to adsorbed molecules, takes place, offering new insights into the early stages in the activation of small molecules.[12−14]

Particular attention has been devoted to the nature and reactivity of the surface anion vacancies with trapped electrons (F_S color centers), whose presence may be experimentally detected by electron paramagnetic resonance (EPR)[11,15−17] or by optical spectroscopies.[18,19] The physics and chemistry of these sites have been explored. The centers are usually formed by addition of low ionization energy metals or by UV irradiation in hydrogen atmosphere. The former technique generates surface F_S and F_S^+ centers, while using UV irradiation in the presence of H_2 creates surface $F_S(H)^+$ centers.

$F_S(H)^+$ centers can be regarded simply as color centers characterized by a distinctive superhyperfine interaction between the trapped electron and a proton from a neighboring surface hydroxyl group. The structure and the mechanism of formation of these centers have been recently characterized using a combined EPR and quantum chemical approach[11,20] starting from the interpretation of the experimental data obtained originally by Tench and co-workers.[15] In the first step, H_2 molecules are adsorbed at the surface in proximity of the vacancy center. The high electric field at this site promotes the activation of the H_2 molecule and causes the heterolytic dissociative chemisorption, with consequent H^+ stabilization on an oxide anion in the proximity of the vacancy (an OH group is indeed formed), while the H^- fragment almost replaces the missing O^{2-} anion at the center of the vacancy ($F_S^{2+}H^+H^-$ intermediate). The H^- fragment is stabilized by the electrostatic interaction with the crystalline potential.[20] UV radiation promotes dissociation of $H^\bullet$ from the vacancy/H^- complex, leaving one electron trapped in the vacancy with formation of the paramagnetic $F_S(H)^+$ center. Globally, the process can be summarized as follows:

$$F_S^{2+} + H_2 \rightarrow [F_S^{2+}\cdots H_2]^{\#} \rightarrow F_S^{2+}H^+H^- + h\nu \rightarrow F_S(H)^+ + H^\bullet \quad (1)$$

However, the existing literature[11,15,20] on $F_S(H)^+$ centers doesn't address the properties of these defects exhaustively. Ab initio calculations were performed only at the Hartree−Fock (HF) level without inclusion of electron correlation, and the possibility of different localization of the OH group was considered only in a schematic way without allowing any geometrical relaxation. Moreover, the electronic structure was discussed only in terms of EPR properties without computing infrared (IR) vibrations, and the reactivity of $F_S(H)^+$ centers was never addressed with quantum chemical methods.

Color centers give rise to charge-transfer reactions when interacting with gas-phase molecules.[13,14,21,22] EPR studies have clearly shown that exposure of a MgO surface with a high concentration of F_S centers to O_2 and N_2 molecules results in

* Corresponding author. E-mail address: aferrari@ch.unito.it.
[†] Università di Milano-Bicocca e Istituto Nazionale per la Fisica della Materia.
[‡] Università di Torino.

10.1021/jp011679b CCC: $20.00 © 2001 American Chemical Society
Published on Web 09/15/2001

the formation of stable or metastable radical anions, O_2^- and N_2^-, respectively,[14,21−25] according to the general reaction:

$$F_S^+ + X_2 \rightarrow F_S^{2+} + X_2^- \quad (2)$$

The formation of the X_2^- species ($X_2 = O_2$, N_2) has been unambiguously demonstrated by the analysis of both the **g** tensors and the hyperfine structures, and the nature of the interaction has been clarified theoreticallly.[14] In both cases, a net charge transfer from the vacancy to the adsorbed molecule occurs: O_2 removes the electron from the MgO oxygen vacancies with an exothermic reaction, forming an adsorbed superoxide anion O_2^- which is stable even at room temperature, while N_2^- is reversibly formed on the surface only at low temperature. However, the observed magnetic equivalence of the two nuclei of X_2 has not been theoretically confirmed, since the corresponding geometric configuration did not result to be favored.[21] Notice that the reported calculations treated only F_S^+ centers while EPR spectra show unambiguously the presence of $F_S(H)^+$ centers. The effect of an OH group adjacent to the vacancy site on the orientation of the adsorbed molecule and on the charge-transfer mechanism has never been addressed computationally.

The aim of the present paper is to characterize the properties and reactivity of $F_S(H)^+$ centers. In particular, we focus on
1. the electronic structure of $F_S(H)^+$ centers, taking into account (i) electron correlation, (ii) geometry relaxation, (iii) different arrangements of the OH group, and (iv) EPR coupling matrix and IR vibrations,
2. verifying if the charge-transfer mechanism observed for F_S^+ centers is still valid in the case of $F_S(H)^+$ centers, and
3. clarifying if the presence of $F_S(H)^+$ centers, instead of F_S^+ ones, at the MgO (001) surface stabilizes a particular configuration of the admolecule.

2. Computational Method

The interaction of N_2 and O_2 with paramagnetic five-coordinated $F_S(H)^+$ centers on the (001) MgO surface has been studied with cluster models, chosen to be sufficiently large to accommodate all significant chemical effects associated with the investigated phenomenon. This method has been widely used to study the adsorption and reaction of molecules with oxide surfaces.[26] The clusters have been embedded in a large array of point charges ±2, the anions at the cluster border being surrounded by an effective core potential (ECP), following a procedure described in ref 21. The clusters adopted to describe the two different $F_S(H)^+$ centers at the MgO surface are denominated [$HO_{12}Mg_5ECP_{25}$] (Figure 1). Ions, ECPs, and PCs taken together are electrically neutral.

For the calculations, we have adopted the gradient-corrected B3-LYP density functional built up by the Becke's three-parameter hybrid exchange functional[27] in combination with the correlation functional of Lee, Yang, and Parr.[28] A tendency of DFT approaches to delocalize in same cases the spin density has been reported;[29] this effect is due to the self-interaction problem,[30] which induces the unpaired electron to delocalize over many atoms in order to reduce the Coulomb repulsion. In this respect, the HF method does not have this problem, as the self-interaction part of the Coulomb energy cancels that of the exchange part. Therefore, in some cases, another hybrid approach, HF-LYP (exchange interaction described at Hartree−Fock level and the correlation part by the LYP correlation functional), has been also adopted. Gaussian-type atomic orbital basis sets have been used to construct the Kohn−Sham orbitals.

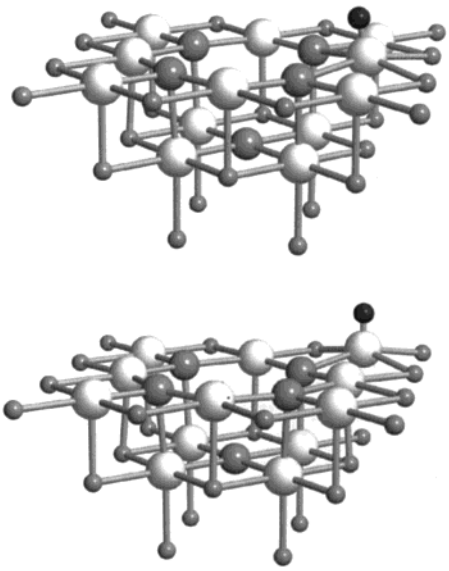

Figure 1. Cluster models of $F_S(H)^+$ centers ($HO_{12}Mg_5ECP_{25}$). (a) $F_S(H_a)^+$: the proton sits on an oxygen atom first neighbor to the vacancy. (b) $F_S(H_b)^+$: the proton sits on an oxygen atom second neighbor to the vacancy. White spheres, O^{2-}; gray spheres, Mg^{2+}; small gray spheres, ECP; small black spheres, H.

In line with previous results,[13,21] no floating functions have been added in the center of the vacancy. The basis sets are the following: H, 6-31G**; Mg, 6-31+G; O first layer, 6-311G, and O second layer, 6-31G. For N_2 and O_2, we have chosen the 6-311+G** basis set, which provides a good estimation of the electron affinity of both molecules.[21]

The geometry of adsorbed admolecules has been fully optimized by means of analytical gradients within the constraint of C_s symmetry. In the MgO clusters, the hydrogen atom, all the magnesium, and the oxygen ions of the first layer were free to move, while the positions of all the other atoms were kept fixed at bulk values. Only the rotational profile reported in the following section has been computed without relaxing the substrate MgO cluster ions.

The binding energies, D_e, have been corrected by the basis set superposition error (BSSE) by applying the standard counterpoise method.[31] The calculations have been performed employing the GAUSSIAN98 program package.[32]

3. Results and Discussion

3.1. Structure and Properties of $F_S(H)^+$. Two different $F_S(H)^+$ centers are the most easily conceived final products of reaction 1: the H^+ fragment is bound to an oxygen anion first neighbor with respect to the vacancy site ($F_S(H_a)^+$, Figure 1a), or the H^+ is placed on a second neighbor oxygen ($F_S(H_b)^+$, Figure 1b). According to reaction 1, the formation energy of $F_S(H_a)^+$ and $F_S(H_b)^+$ centers differ by less than 0.2 eV at the B3LYP level. However, a reaction process connecting reactants and products along the path described in (1) has been easily determined only for $F_S(H_a)^+$. At the B3-LYP level, a transition state has been found with an activation energy of 0.58 eV with respect to the F_S^{2+}/H_2 complex, not far from the value of 0.87 eV calculated in a previous work without including correlation;[20] the transition state is characterized by a considerable elongation of the bond distance of H_2 (d(H−H) = 0.954 Å compared with 0.732 Å for free H_2), accompanied by an incipient formation of the O−H bond (d(O−H) = 1.348 Å). The heterolytic dissociation of the H−H bond occurs via the formation of the

adduct $F_SH^+H^-$: we find this intermediate to be more stable than the F_S^{2+}/H_2 complex by 0.66 eV at B3-LYP level, at variance with previous calculations.[20] The reasons for this discrepancy are various: (i) different method and level of calculation and (ii) different degree of geometry relaxation. The intermediate $F_SH^+H^-$ has been characterized spectroscopically. The computed IR vibrations (O−H stretching mode ν(OH) = 3703 cm^{-1}, OH bending δ(OH) = 814−887 cm^{-1}, vibrations involving H^- $\nu(H^-)$ = 994−1000 cm^{-1}) compare well with experimental observations (ν(OH) = 3712 cm^{-1}, δ(OH) = 889 cm^{-1}, $\nu(H^-)$ = 1125 cm^{-1})[35,24] (see Table 2). Although the formation of $F_S(H_b)^+$ is likely on the basis of thermodynamic considerations, a direct reaction path leading to the formation of this species could not be located: a more complicate reaction mechanism must be invoked, probably involving migration of H fragment on the MgO surface.

The geometrical structure of $F_S(H_a)^+$ and $F_S(H_b)^+$ centers is characterized by an outward motion of the Mg^{2+} adjacent to the vacancy and in the opposite direction with respect the −OH group because of the positive electrostatic potential generated by the proton; on the contrary, the first neighbor O^{2-}'s move inward. The main result is a slight shrinkage of the Mg−O distances adjacent to the vacancy site and a moderate elongation for distances close to the −OH group; computed Mg−O distances vary from 1.91 to 2.11 Å and from 2.05 to 2.21 Å for the $F_S(H_a)^+$ and $F_S(H_b)^+$ centers, respectively (bulk value 2.104 Å).[33]

Both $F_S(H_a)^+$ and $F_S(H_b)^+$ are characterized by a polarization of the spin density induced by the proton (Figure 2). Computed EPR hyperfine coupling constants of the unpaired electron with the ^{25}Mg nuclide confirm the spin polarization. The main contribution to the hyperfine coupling matrix **A** is due to the isotropic part, a_{iso}, or Fermi contact term; a_{iso} values can be related to the amount of unpaired electron delocalized at the 3s Mg^{2+} orbital. At the B3-LYP level, the two Mg^{2+} centers adjacent to the OH group of the $F_S(H_a)^+$ center have a value of a_{iso} = −11 G, at least 10 times larger than the values of the other cations of the cavity (Figure 1 and Table 1). The hydroxyl group experiences the presence of the entrapped spin as indicated by the geometrical structure (the OH bond is slightly bent in the direction of the vacancy, Figure 1) and by the spin density distribution (a small amount of spin density is delocalized at the H nucleus giving rise to the super-hyperfine coupling of the EPR spectra: a_{iso}(H) = 1.8 G, Table 1). These findings are consistent with previous HF calculations and indicate that as well as F_S^+ sites, $F_S(H)^+$ centers are characterized by a spin distribution almost completely localized at the center of the vacancy. B3-LYP and HF-LYP results are fully comparable and in excellent agreement with the observed EPR data (Table 1).

Similarly, in the $F_S(H_b)^+$ center, the spin density is delocalized only for ∼11% at the Mg^{2+} cation close to the OH group. Almost no interaction between the OH group and the unpaired electron can be identified in this case. This suggests that the proton must be very close to the vacancy in order to give rise to the typical EPR spectrum of the $F_S(H)^+$ centers and to the superhyperfine interaction. However, the two color centers, $F_S(H_a)^+$ and $F_S(H_b)^+$, are compatible with the heterogeneity of the EPR spectrum, which shows the existence of two species, one characterized by the super-hyperfine coupling between the trapped electron and the adjacent proton and one in which this coupling is absent. Unfortunately, in the latter case, the hyperfine profile could not be resolved.[11]

The qualitatively different electronic structure of $F_S(H_a)^+$ and $F_S(H_b)^+$ centers is also manifested by the IR vibrations; the calculated O−H stretching vibration in $F_S(H_a)^+$, ν(OH) = 3630 cm^{-1}, is lower than that for $F_S(H_b)^+$, ν(OH) = 3703 cm^{-1}, and the corresponding IR intensity is enhanced by more than a factor 3 (I = 134 and 40 km mol^{-1} for $F_S(H_a)^+$ and $F_S(H_b)^+$),

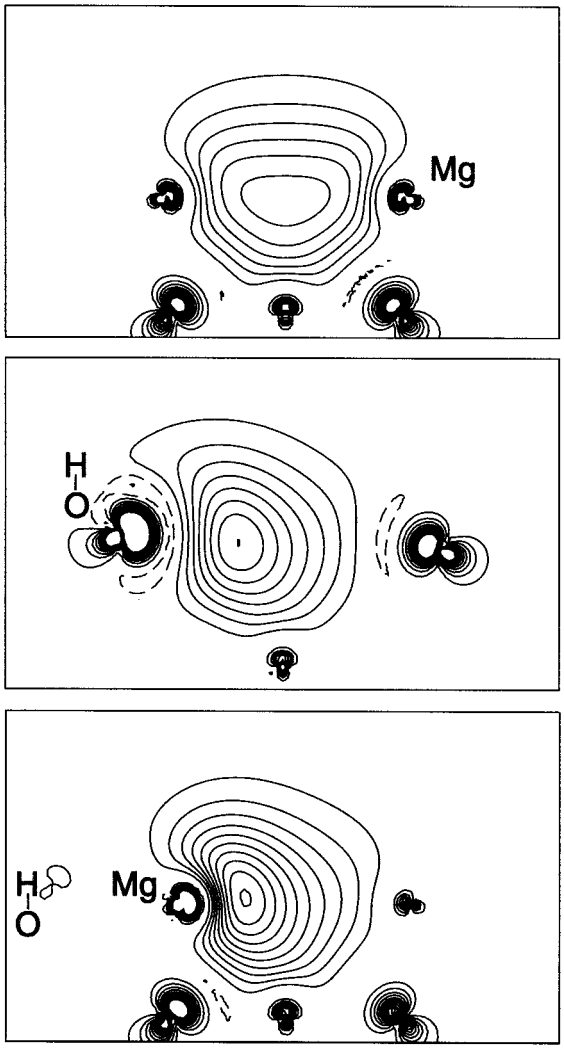

Figure 2. Isocontour lines of the spin density for (a) F_S^+, (b) $F_S(H_a)^+$, and (c) $F_S(H_b)^+$ centers computed at B3-LYP level. The contour lines are drawn in a plane normal to the MgO surface at intervals of 0.001 |e|/bohr^3.

TABLE 1: Values of EPR Hyperfine Coupling Matrix (A = a_{iso} + B) for the Paramagnetic $F_S(H_a)^+$, $F_S(H_b)^+$, and F_S^+ Centers[a]

		Mg^{first}	Mg^{second}	Mg^{third}	Mg_{second_layer}	H
$F_S(H_a)^+$	a_{iso}	−11.2 (−11.1)	−0.9 (−0.7)	−	−2.3 (−3.7)	−1.8 (−3.0)
	A_1	−10.4 (−10.1)	−0.7 (−0.4)	−	−2.0 (−3.3)	−4.7 (−5.9)
	A_2	−10.4 (−10.2)	−0.7 (−0.5)	−	−2.0 (−3.3)	−2.0 (−3.3)
	A_3	−12.8 (−12.9)	−1.3 (−1.1)	−	−2.9 (−4.5)	1.3 (0.2)
$F_S(H_b)^+$	a_{iso}	−20.0	−3.7	−1.1	−3.3	−0.05
	A_1	−19.0	−3.3	−0.9	−3.8	0.35
	A_2	−19.0	−3.3	−0.9	−3.5	0.35
	A_3	−22.0	−4.5	−1.5	−2.6	−0.75
F_S^+	a_{iso}	−5.1	−	−	−3.8	−
	A_1	−4.64	−	−	−3.5	−
	A_2	−4.74	−	−	−3.5	−
	A_3	−6.04	−	−	−4.5	−
exp.[b]	$A_\perp$	10.5	0.73	−	−	2.07
	$A_\parallel$	11.4	0.75	−	−	0.4

[a] See also Figures 1 and 2 (B3-LYP results,HF-LYP values in parentheses). All data in Gauss. The labels first, second, and third refer to the position of Mg cations with respect the OH group. [b] Observed EPR data from ref 11.

TABLE 2: Harmonic Vibrational Frequencies of an OH Group near an Oxygen Vacancy at the (001) Surface of MgO, $F_S(H)^+$, and of an O_2 Molecule Adsorbed on the Vacancy, $F_S(H_a)^{2+}/O_2^-$ (B3-LYP results)[a]

vibrational mode	$F_S(H_a)^+$	$F_S(H_b)^+$	$F_S(H_a{}^+H^-)$	$F_S(H_a)^{2+}/O_2^-$ A	B	C
OH stretching, ν(OH)	3630	3703	3743	3727	3769	3661
OH bending (parallel to the vacancy), δ(OH)	830	938	826	967	824	947
OH bending (toward the vacancy), δ (OH)	822	833		865	840	901
H^- vertical stretching, $\nu(H^-)$			887, 814[b,d]			
H^- motion in the vacancy plane			1008, 994[d]			
O_2^- stretching,[c] ν(O−O)				1175	990	1098

[a] All values are in cm^{-1}. Experimental values from refs 24, 34, and 35. [b] Mixed vibration (OH bending and H^- stretching). [c] ν(O−O) for isolated O_2^- 1165 cm^{-1}. [d] Corresponding values for $F_S{}^{2+}/H^-$ system (without nearby proton) are 1005 and 878 cm^{-1}.

respectively (Table 2). The red shift of the OH stretching vibration in $F_S(H_a)^+$ and the concomitant increment of the IR intensity with respect to $F_S(H_b)^+$ are typical of hydrogen bonding; the existence of a special kind of hydrogen-bond interaction between the OH group and the trapped electron, already reported,[34] has been theoretically confirmed. Both stretching frequencies match the experimental observations: the IR spectra indicate the presence of several OH species; among them, one can be attributed to an isolated OH group (ν(OH) = 3712 cm^{-1}) and another one to hydroxyl species probably involved in hydrogen bonding interactions and red shifted by almost 80−110 cm^{-1}.[24,34,35]

The ionization potentials (IP) of both $F_S(H_a)^+$ and $F_S(H_b)^+$ centers are similar (IP($F_S(H_a)^+$) = 10.8 eV and IP($F_S(H_b)^+$) = 10.1 eV at B3-LYP level); the values are about 4.2 eV higher than that computed for the $F_S{}^+$ site. This is due to the presence of an additional positive charge, that of the proton, which enhances the positive electrostatic potential at the vacancy site. However, because of the intrinsic limitations of the model, charged cluster, and the lack of long-range polarization, these results do not provide a quantitative estimate of the ionization energy.

3.2. Reactivity of $F_S(H)^+$. Despite the higher ionization potential, $F_S(H)^+$ centers show a similar reactivity as the $F_S{}^+$ ones: in fact, when N_2 and O_2 molecules interact with these sites, a charge transfer from the surface to a π^* antibonding orbital of the admolecule occurs. Three stationary points in the potential energy surface have been localized for the charge-transfer species, corresponding to different configurations (Figure 3). The main features of the $F_S(H_a)^{2+}/O_2^-$ and $F_S(H_a)^{2+}/N_2^-$ surface complexes are reported in Table 3. Orientation A of the $F_S(H_a)^{2+}/O_2^-$ complex is slightly less stable than orientations B and C. At the B3-LYP level, the preferred structure is the B one: however, in this case, the unpaired electron results to be partially delocalized over the O^{2-} surface anion facing the vacancy and closest to the admolecule. Such a spin distribution is not found in a HF-LYP calculation (Table 3) and can be indeed regarded as an artifact induced by the DFT method (see also the Computational Details section).[29,30] In fact, the problem disappears at HF-LYP level, where orientations B and C have a similar stability, even if HF-LYP binding energies seem to be slightly overestimated with respect to B3-LYP values, Table 3.

The two more stable structures, B and C, have different electronic ground states, $^2A''$ and $^2A''$, respectively, as a result of the occupation of the two components of the π^* orbital (Table 3). For this reason and despite the small difference in stability, a fluxional behavior between these two forms implies a crossing of the two states and the rupture of the local symmetry. Note that, like in the case of N_2, the extra electron in the O_2^- radical prefers the π^* a″ orbital perpendicular to the symmetry plane for orientation B and the π^* a′ orbital in the symmetry plane

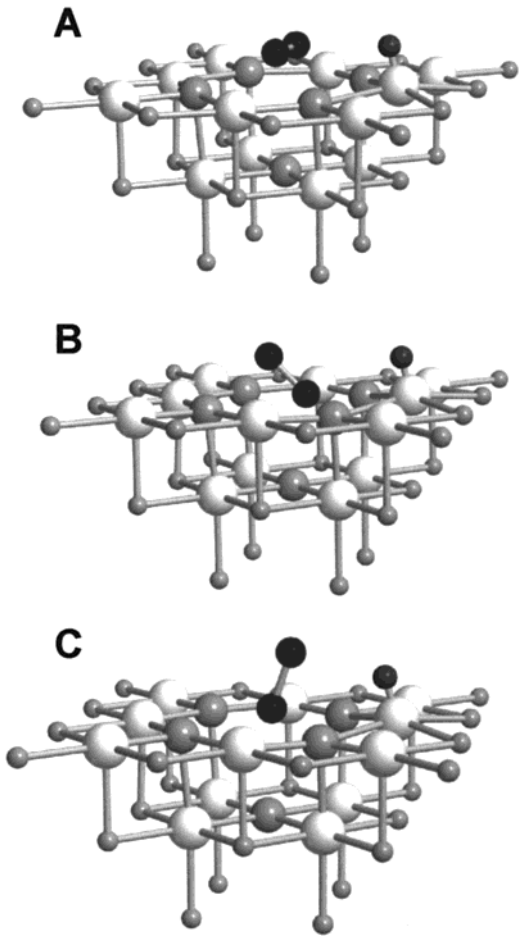

Figure 3. Schematic representation of the different orientations (A, B, and C) of the $F_S(H_a)^{2+}/X_2^-$ (X = N, O) complexes considered in this study. White spheres, O^{2-}; gray spheres, Mg^{2+}; small gray spheres, ECP; large black spheres, N and O; small black spheres, H.

for orientation C. On the contrary, structure A has the extra electron located in the π^* a′ orbital parallel to the surface which spans an a′ symmetry when the molecule adopts a vertical configuration. Therefore, orientation A has the same electronic structure as orientation C: the rotational profile (Figure 4) suggests structure A as a transition state in the process of surface rotation between two equivalent C configurations. This consideration is supported by frequency calculation. Structure A is characterized by an extra negative frequency. Inspection of this vibrational mode indicates a tendency of the molecule to move from orientation A, parallel to the surface, to a tilted arrangement, C. Moreover, a direct search for such a transition state leads again to structure A. This let us conclude that the rotation of adsorbed O_2^- radicals is hindered at low temperature. Given

TABLE 3: Main Properties of the Charge Transfer Complexes $F_S(H)^{2+}/N_2^-$ and $F_S(H)^{2+}/O_2^-$[a]

	$F_S(H_a)^{2+}/N_2^-$			$F_S(H_a)^{2+}/O_2^-$		
orientation	A	B	C	A	B	C
$z(X_2)$	1.286	0.832	0.759	1.021	0.221 (0.181)	0.380
$r(X-X)$[b]	1.175	1.187	1.188	1.331	1.408 (1.288)	1.362
spin density at X[c]	0.44	0.32/0.56	0.41/0.52	0.47	0.16/0.45[d] (0.18/0.80)	0.28/0.67 (0.16/0.81)
ΔE	−0.20	−0.51	−0.50	−3.27	−3.77 (−4.08)	−3.37 (−4.17)
ΔE (BSSE)	0.37	0.09	0.04	−2.68	−3.11	−2.80
electronic state	$^2A''$ $(a'')^1$ [e]	$^2A''(a'')^1$	$^2A'$ $(a')^1$	$^2A'(a'')^2(a')^1$ [e]	$2A'$ $(a'')^2(a')^1$	$^2A''$ $(a')^2(a'')^1$

[a] Data refer to B3-LYP calculations (HF-LYP values in parentheses). Geometrical parameters in Å; energy differences, ΔE, and BSSE corrected, ΔE(BSSE), relative to the process $F_S(H_a)^{2+}/X_2^- \rightarrow F_S(H_a)^+ + X_2$ (X = O, N), in eV; spin density in au. [b] Gas-phase values (B3-LYP): $N_2 = 1.096$ Å, $N_2^- = 1.180$ Å; $O_2 = 1.206$ Å, $O_2^- = 1.346$ Å; (HF-LYP): $O_2 = 1.146$ Å, $O_2^- = 1.271$ Å. [c] For nonequivalent nuclei, values for the bottom/top atom are given. [d] A spin density 0.4 is found at the O^{2-} lattice anion closest to O_2^- molecule. [e] For orientation A, both π^* orbitals (one perpendicular and one parallel to the surface) span the a'' symmetry. The extra electron in the $F_S(H_a)^{2+}/N_2^-$ and $F_S(H_a)^{2+}/O_2^-$ complexes is localized in the $a''(\pi^*)$ parallel to the surface. Note for clarity that an adsorbed neutral oxygen molecule according to orientation B or C should have the $(a')^1(a'')^1$ electron configuration

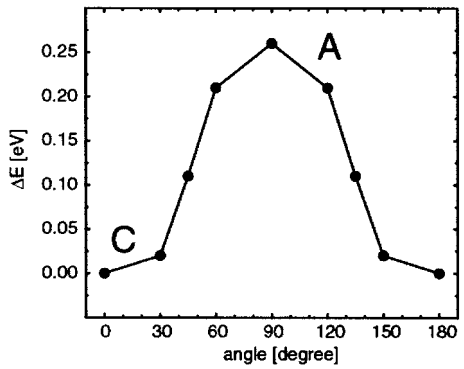

Figure 4. Energy profile for the rotation of O_2^- adsorbed on $F_S(H_a)^{2+}$. The substrate has not been relaxed. The angle is between the plane containing the center of the vacancy and the OH group and the oxygen molecule. 90° corresponds to orientation A; 0° to orientation C.

a rotation barrier of about 0.2 eV, free rotation is expected at room temperature.

Regardless of the orientation assumed, of all configurations are very stable with respect to dissociation into $F_S(H_a)^+$ and O_2 fragments. Analogously to O_2, orientations B and C of $F_S(H_a)^{2+}/N_2^-$ are similar in energy at the B3-LYP level (they differ by less than 0.05 eV), and both are metastable with respect to dissociation into $F_S(H_a)^+$ and N_2 fragments. This small metastability, (0.09 and 0.04 eV for orientations B and C, respectively, Table 2) is fully comparable to that computed for F_S^{2+}/N_2^- complexes (0.1 eV).[21] Despite the minimal difference in stability, configurations B and C localize the unpaired electron in different orbitals (Table 3): the interchange between these two forms requires an electronic transition. Again, structure A has the extra electron located in the π^* a′ orbital parallel to the surface which spans an a' symmetry when the molecule adopts a vertical configuration; therefore, orientation A has same electronic structure as structure C, and for analogy with that reported for the O_2 case, it could be indeed depicted as the transition state in the surface rotation of C oriented admolecules.

We discuss now the main features of the charge-transfer complexes. The computed N−N and O−O distances in the corresponding surface charge-transfer complexes are elongated by about 8−9% compared to those of the gas-phase molecule: this is consistent with the reduced bond order and with the partial activation of the bond, due to the charge transfer of one electron from the surface F center to a π^* antibonding orbital of the admolecule (Table 3). The DFT computed values of the spin density on N_2, 88% for A and B and 92% for the C orientation, respectively, are in excellent agreement with the value of 92% reported in ref 13 from the computer simulated EPR spectrum (Table 3). The values are consistent with an almost complete electron transfer to the N_2 molecule. Similarly, the calculated spin density on O_2, more than 94% for all orientations, demonstrates a complete electron transfer.

Table 4 reports the EPR hyperfine coupling matrix for all orientations of the $F_S(H_a)^{2+} + X_2^-$ surface complexes. For the parallel orientation, the agreement between computed and measured hyperfine constants is excellent.[14,23] For orientations B and C of $F_S(H_a)^{2+}/N_2^-$, the magnetic equivalence of the two N nuclei is lost, and the spin density is mostly localized at the top N nucleus: the considerable magnetic inequivalence of the two nuclei (A_1 differs by about 13 G, see Table 4) is not observed experimentally.[14,23] Like N_2, when O_2^- is adsorbed in orientations B and C, the magnetic equivalence of the two O nuclei is lost, but also in this case, the inequivalence of the two nuclei (Table 4) has not been observed experimentally.[12,21,24] All the components of the hyperfine constant for configuration A and the averaged values for orientations B and C are almost equal to those computed for the free radical anion: they are consistent, indeed, with the EPR analysis that indicates a complete charge transfer.

Structures B and C of adsorbed O_2 or N_2 on $F_S(H)^+$, which have very similar EPR properties, could be in principle discriminated by IR spectroscopy. We have considered in detail the case of O_2 which gives rise to a stable surface complex. Structure C is characterized by a red shift of the O−H stretching frequency with respect to the $F_S(H)^+$ center without adsorbed O_2 (Table 2); also, the O−O stretching vibration is different in orientations B and C (see Table 2). These findings indicate again a sort of hydrogen interaction for structure C where the distance between O−H and O_2^- and the relative orientation of the two fragments is more favorable.

To summarize, we have found that, despite the presence of an hydroxyl group adjacent to the vacancy, the reactivity of $F_S(H_a)^+$ centers toward gas-phase molecules, N_2 and O_2, is similar to that of the F_S^+ sites. The reactivity of $F_S(H_b)^+$ centers, where the OH group is even farther from the vacancy, is also expected to be similar, and has not been considered.

4. Conclusions

The electronic structure of $F_S(H)^+$ centers at the (001) surface of MgO has been investigated by means of theoretical calcula-

TABLE 4: ^{14}N and ^{17}O Hyperfine Coupling Constants for the $F_S(H_a)^{2+}/N_2^-$ and $F_S(H_a)^{2+}/O_2^-$ Complexes as Well as for the Corresponding O_2^- and N_2^- Radical Anions Computed at the B3-LYP Level (HF-LYP Values in Parentheses)[a]

	X = N				X = O			
system[b]	A_1	A_2	A_3	a_{iso}	A_1	A_2	A_3	a_{iso}
X_2^-	18	−6	−6	2	−71 (−105)	17 (−9)	18 (−6)	−12 (−40)
$F_S(H_a)^{2+}/X_2^-$ (A)	19	−6	−7	2	−66	18	19	−10
$F_S(H_a)^{2+}/X_2^-$ (B)[c]	24	−8	−7	3	−66 (−134)	21 (5)	21 (6)	−7 (−49)
$F_S(H_a)^{2+}/X_2^-$ (B)[d]	14	−6	−5	1	−25 (−49)	7 (−5)	5 (−3)	−4 (−19)
$F_S(H_a)^{2+}/X_2^-$ (C)[c]	26	−6	−5	5	−85 (−136)	27 (6)	28 (7)	−10 (−41)
$F_S(H_a)^{2+}/X_2^-$ (C)[d]	15	−5	−4	2	−48 (−44)	11 (−6)	12 (−4)	−8 (−18)
MgO/X_2^- [e]	22	−3	−4	5	±77	∼0	∼0	−

[a] All values in Gauss [b] In parentheses are the orientations of the adsorbed molecule. See also Figure 3. [c] Data concerning the top atom of X_2^-. [d] Data concerning the bottom atom of X_2^-. [e] Experimental values from ref 23 (N_2) and 22 (O_2).

tions. Two different arrangements of the OH group on the surface have been considered, $F_S(H_a)^+$ and $F_S(H_b)^+$: they differ for the position of the proton which sits on a oxygen atom first or second neighbor of the anion vacancy, respectively. The computed properties are in general agreement with observed EPR and IR data and show the existence of important analogies between the two arrangements but also of some significant differences. Both centers are characterized by the same formation energy and ionization potential and by a similar polarization of the spin density induced by the presence of the hydroxyl group. Some specific aspects of the EPR super-hyperfine coupling constant, the OH stretching vibration, and the geometrical structure suggest the existence of a special kind of hydrogen bond between the OH group and the trapped electron in $F_S(H)^+$. However, although a direct reaction path connecting reactants and products according to reaction 1 could be identified only for $F_S(H_a)^+$ sites, both $F_S(H_a)^+$ and $F_S(H_b)^+$ centers are compatible with the IR and EPR observations.

The presence of the OH group in proximity of the oxygen vacancy results in a different electronic structure from that of F_S^+ centers. Despite their peculiar properties, reactivity of $F_S(H_a)^+$ and F_S^+ centers is comparable. At short distances from these sites, both O_2 and N_2 molecules extract the electron trapped in the cavity, leading to a stable radical anion (O_2^-) or to a metastable species (N_2^-), according to the propensity of the molecule to accommodate one extra electron. The charge-transfer complexes are stabilized by the electrostatic interaction between the charged fragments: $F_S(H_a)^{2+}$or $-F_S^{2+}$ and O_2^- or N_2^-. The different behavior of the two molecules is consistent with experimental observations: O_2^- is formed irreversibly and is stable even at room temperature, while N_2^- is reversibly formed only at low temperature (77 K).

According to the calculations the more stable configurations of the charge-transfer complexes $F_S(H_a)^{2+}/O_2^-$ and $F_S(H_a)^{2+}/N_2^-$ are characterized by a magnetic inequivalence of the two atoms of the admolecule. The hypothesis that an OH group near the vacancy site could energetically favor a parallel orientation of the molecule where the two nuclei are equivalent, as observed experimentally (see, e.g., structure A in Figure 3) is not supported by the present results. In particular we found that structure A is a transition state in the rotational motion of the adsorbed radical anions. The small barrier could result in a fluxional behavior of the admolecule at temperatures above the liquid nitrogen, thus explaining the magnetic equivalence. However, this consideration fails on observing that the spectra of N_2 were recorded cooling the sample at the liquid He temperature, without any substantial modification.[23]

In syntheses, we have described a surface defect, the $F_S(H)$ center, which fits extremely well with the EPR experimental evidences. However, when considering its interaction with small molecules (i.e., O_2 and N_2), the agreement with the experimental observations is lost as far as the magnetic equivalence of the two nuclei is concerned. We think that $F_S(H)$ centers described in this work contribute to the EPR spectra, but they probably constitute only a minor part of the signal. In this respect, it should be noted that the calculations treated only $F_S(H)^+$ centers located at the (001) terrace of MgO: actually, the experimental and computational evidences concerning the high heterogeneity of defect sites at the MgO surface are very numerous. F_S and $F_S(H)$ centers can be located at low-coordinated sites[11] (edge, corner, step, kinks) and other centers beside the oxygen vacancies can act as electron traps (for instance the site generated by removing a neutral MgO unit).[36] Formation of such electron traps is energetically less expensive than when they are located at the (001) regular surface, and they could be the most abundant defect sites present at the MgO surface.[3,11,36] It is indeed likely that the EPR spectra may be mainly due to these centers characterized by a higher degree of coordinative unsaturation of the exposed ions which might favor a parallel orientation of the N_2^- and O_2^- anions.

Acknowledgment. The authors would like to thank Prof. E. Giamello for useful comments and for critical reading of the manuscript. A. M. F. is grateful to B. Civalleri for helpful discussions. The financial support of the INFM through the PRA-ISADORA project and of the Ministry of University and Research (MURST) through the National Program: "Strati ultrasottili di ossidi e solfuri inorganici: crescita, caratterizzazione e reattività superficiale" is gratefully acknowledged.

References and Notes

(1) Colbourn, E. A. *Surf. Sci. Rep.* **1992**, *15*, 281.
(2) Shluger, A. L.; Gale, J. D.; Catlow, C. R. A. *J. Phys. Chem*. **1992**, *96*, 10389.
(3) Ferrari, A. M.; Pacchioni, G. *J. Phys. Chem.* **1995**, *99*, 17010.
(4) Pelmenschikov, A. G.; Morosi, G.; Gamba, A.; Coluccia, S. *J. Phys. Chem. B* **1998**, *102*, 2226.
(5) Scorza, E.; Birkenheuer, U.; Pisani, C. *J. Chem. Phys*. **1997**, *107*, 9645.
(6) Pacchioni, G.; Pescarmona, P. *Surf. Sci*. **1998**, *412/413*, 657.
(7) Sushko, P. V.; Shluger, A. L.; Catlow, C. R. A. *Surf. Sci*. **2000**, *450*, 153.
(8) Pacchioni, G. *Surf. Rev. Lett.* **2000**, *7*, 277.
(9) Tench, A. J.; Holroyd, P. *Chem. Comm*. **1968**, 471.
(10) Che, M.; Tench, A. J. *J. Adv. Catal*. **1983**, *32*, 1.
(11) Giamello, E.; Paganini, M. C.; Murphy, D. M.; Ferrari, A. M.; Pacchioni, G. *J. Phys. Chem*. **1997**, *101*, 971.
(12) Giamello, E.; Murphy, D. M.; Marchese, L.; Martra, G.; Zecchina, A. *J. Chem. Soc., Faraday Trans*. **1993**, *89*, 3715.
(13) Giamello, E.; Murphy, D. M.; Garrone, E.; Zecchina, A. *Spectrochim. Acta* **1993**, *49A*, 1323.
(14) Chiesa, M.; Giamello, E.; Paganini, M. C.; Pacchioni, G.; Soave, R.; Murphy, D. M.; Sojka, Z. *J. Phys. Chem. B* **2001**, *105*, 497.
(15) Tench, A. J.; Nelson, R. L. *J. Colloid Interface Sci*. **1968**, *26*, 364.
(16) Tench, A. J. *Surf. Sci*. **1971**, *25*, 625.

(17) Giamello, E.; Murphy, D. M.; Ravera, L.; Coluccia, S.; Zecchina, A. *J. Chem. Soc., Faraday Trans*. **1994**, *90*, 3167.
(18) Wu, M. C.; Truong, C. M.; Coulter, K.; Goodman, D. W. *J. Am. Chem. Soc*. **1992**, *114*, 7565.
(19) Peterka, D.; Tegenkamp, C.; Schroeder, K. M.; Ernst, W.; Pfnür, H. *Surf. Sci*. **1999**, *431*, 146.
(20) D'Ercole, A.; Giamello, E.; Pisani, C. *J. Phys. Chem*. **1999**, *103*, 3872.
(21) Ferrari, A. M.; Soave, R.; D′Ercole, A.; Pisani, C.; Giamello, E.; Pacchioni, G. *Surf. Sci*., in press.
(22) Pacchioni, G.; Ferrari, A. M.; Giamello, E. *Chem. Phys. Lett*. **1996**, *255*, 58.
(23) Giamello, E.; Paganini, M. C.; Chiesa, M.; Murphy, D. M.; Pacchioni, G.; Soave, R.; Rockenbauer, A. *J. Phys. Chem. B* **2000**, *104*, 1887.
(24) Paganini, M. C.; Chiesa, M.; Giamello, E.; Coluccia, S.; Martra, G.; Murphy, D. M.; Pacchioni, G. *Surf. Sci*. **1999**, *421*, 246.
(25) Ferrari, A. M.; Pacchioni, G. J. *Chem. Phys.* **1997**, *107*, 2066.
(26) In *Cluster Models for Surface and Bulk Phenomena*; NATO ASI Series B; Pacchioni, G., Bagus, P. S., Parmigiani, F., Eds.; Plenum: New York, 1992; Vol. 283.
(27) Becke, A. D. *J. Chem. Phys.* **1993**, *98*, 5648.
(28) Lee, C.; Yang, W.; Parr, R. G. *Phys. Rev. B* **1988**, *37*, 785.
(29) Pacchioni, G.; Frigoli, F.; Ricci, D.; Weil, J. A. *Phys. Rev. B* **2001**, 54102.
(30) Parr, R. G.; Yang, W. *Density Functional Theory of Atoms and Molecules*; Oxford Science Publications: Oxford, 1989.
(31) Boys, S. F.; Bernardi, F. *Mol. Phys.* **1970**, *19*, 553.
(32) Frisch, M. J.; et al. *Gaussian 98*; Gaussian Inc.: Pittsburgh, PA, 1998.
(33) Wyckoff, R. W. G. *Crystal Structure*; Interscience: New York, 1965.
(34) Diwald, O.; Knozinger, E.; Martra, G. *J. Chem. Phys.* **1999**, *111*, 6668.
(35) Knozinger, E.; Jacob, K. H.; Hofmann, P. *J. Chem. Soc., Faraday Trans*. **1993**, *89*, 1101.
(36) Ojamäe, L.; Pisani, C. *J. Chem. Phys*. **1998**, *109*, 10984.